Journal of Sound and Vibration (1999) **226**(2), 217–235
Article No. jsvi.1999.2295, available online at http://www.idealibrary.com on IDEAL®

DAMAGE DETECTION IN BRIDGES USING MODAL CURVATURES: APPLICATION TO A REAL DAMAGE SCENARIO

M. M. Abdel Wahab

School of Mechanical & Materials Engineering, University of Surrey, Guildford GU25XH, U.K.

AND

G. De Roeck

Department of Civil Engineering, KU Leuven, Belgium

(*Received* 8 *January* 1999, *and in final form* 23 *March* 1999)

Damage detection in civil engineering constructions using the dynamic system parameters has become an important research topic. A direct, fast and inexpensive method is therefore required to evaluate and localize damage using the change in dynamic parameters between the intact and damage states. This paper investigates the application of the change in modal curvatures to detect damage in a prestressed concrete bridge. To establish the method simply supported and continuous beams containing damaged parts at different locations are tested using simulated data. Some important conclusions concerning the computation of the modal curvatures are drawn. A damage indicator called "curvature damage factor" is introduced, in which the difference in curvature mode shape for all modes can be summarized in one number for each measured point. The technique is further applied to a real structure, namely bridge Z24 which lies between the villages Koppigen and Utzenstorf and crosses the highway A1 between Bern and Zurich in Switzerland. In the framework of a Brite-Euram project, the bridge is used as a full-scale specimen and subjected to different damage scenarios in order to introduce damage.

1. INTRODUCTION

The problem of maintenance and repair of existing civil engineering structures involves detection of damage at an early stage. The cost of repair is obviously less than tht required to reconstruct the whole structure. Visual inspection technique has a limited capability to detect damage, especially when damage lies inside the structure and is not visible. During the last decade, the use of the dynamic system parameters such as natural frequencies, damping ratio and mode shapes to detect damage qualitatively and quantitatively has been studied intensively. The reason of this popularity is the ease of measuring modal parameters on real structures. The natural frequencies and the mode shapes are directly related to the stiffness of the

0022-460X/99/370217 + 19 $30.00/0

structure. Therefore, a drop in natural frequencies or a change in mode shapes will indicate a loss of the stiffness. As cracks create new surfaces, the damping ratio will increase when damage progresses in the structure.

The change in natural frequencies and damping ratios can easily indicate the presence of damage or faults and its severity. Applications of this concept have been reported in the literature such as damage detection in composite materials [1] and in off-shore structures [2, 3]. For a better localization of damage other dynamic parameters have been proposed: power spectral densities [4] and curvature of mode shapes [5] which showed more sensitivity to damage than the mode shapes themselves. Application of this method to bridges has been reported in the literature by many researchers, e.g. Williams and Salawu [6], Sikorsky and Stubbs [7] and Farrar and Jauregai [8].

The above technique is called "the response-based approach" since the response data are directly related to damage. This approach is therefore fast and inexpensive. Another method known as "the model-based approach" [9–13] has been proposed to detect damage based on updating certain parameters to get perfect agreement between the experimental measured modal parameters and an initial finite element model. The updated parameters can be used afterwards to evaluate damage and identify its location. The drawback of such a method lies in the requirement of reducing the numerical model or extending the measured modal parameters. This is due to the fact that not all degrees of freedom in the numerical model can be measured because of practical reasons. This second approach is more expensive and time consuming than the former approach. However, the latter approach is more suitable for complex structures. An excellent textbook discussing the updating techniques and their applications is due to Friswell and Mottershead [14].

This paper deals with the first technique and its application to a prestressed concrete bridge. The paper of Pandey *et al.* [5] shows a quite interesting phenomenon: that is, the modal curvatures are highly sensitive to damage and can be used to localize it. They used simulated data for a cantilever and a simply supported beam model to demonstrate the applicability of the method. The damaged beam was modelled by reducing the E-modules of a certain element. By plotting the difference in modal curvature (MC) between the intact and the damaged case, a peak appears at the damaged element indicating the presence of a fault. They used a central difference approximation to derive the curvature mode shapes from the displacement mode shapes. An important remark could be observed from the results of Pandey *et al.* [5]: that is, the difference in MC between the intact and the damaged beam showed not only a high peak at the fault position but also some small peaks at different undamaged locations for the higher modes. This can cause confusion to the analyst in a practical application in which one does not known in advantage the location of faults. The first part of this paper is concerned with investigation of the accuracy when using the central difference approximation to compute the MC and determine the reason of the presence of the misleading small peaks. The application of the technique to constructions in which more than one fault positions exist is further investigated using a continuous beam with simulated data. To summarize the results of different modes in one number,

a damage indicator called "Curvature Damage Factor" (*CDF*) is introduced based on averaging the difference in *MC* for all modes. In the second part of this paper, the technique described above is applied to prestressed concrete bridge, Z24. In the framework of the Brite-Euram project BE 96-3157 [15], SIMCES, "System Identification to Monitor Civil Engineering Structures", Progressive Damage Tests (PDT) are applied to a prestressed concrete bridge (Z24) in Switzerland. The intention is to make use of a full-scale proof in order to validate the use of vibration monitoring for the purpose of damage detection and evaluation. After finishing the PDT, the Z24 bridge should be demolished to give way to a railway infrastructure project. The Z24 is replaced by a new bridge (A36). The damage scenarios applied to bridge Z24 are [16]: settlement of pier, tilt of foundation, spalling of concrete, land slide, cut of concrete hinges at abutments, failure of anchor heads of post-tensioning wires and failure of post-tensioning wires. The damage scenarios that are applied to the bridge Z24 have been simulated numerically in reference [17] in order to predict in advance the change in modal parameters after each scenario. It was possible to predict when and where cracks would be initiated by each scenario. A complete description of the finite element model of the bridge can be found in reference [18]. Some of the scenarios introduce damage in the bridge and others introduce change in boundary conditions (structure/soil stiffnesses). The scenario that introduces pronounced damage in the bridge girder is the settlement of pier. The results of this scenario will be analyzed in this paper and damage will be detected and localized by using the measured change in modal curvatures.

2. SIMULATED DATA

2.1. SIMPLE BEAM

The easiest way to compute the modal curvatures (*MC*) from the mode shapes makes use of the central difference approximation, i.e.,

$$v'' = \frac{(v_{i+1} - 2v_i + v_{i-1})}{h^2}, \tag{1}$$

where h is the distance between two successive measured locations.

A simply supported finite element beam model is constructed using 20 beam elements as shown in Figure 1. This model is similar to that studied by Pandey *et al.* [5]. For the intact beam, a constant stiffness *EI* is assumed for all elements, while the damaged beam is modelled by reducing *EI* of the element at the middle of the beam (element 10) by 90%. This high reduction in *EI* is chosen herein because in the study of Pandey *et al.* [5], some small peaks have been observed in the difference between the *MC* of the intact and the damaged be in the undamaged parts of the beam for 90% reduction in *EI* at element 10 (Figure 11 in reference [5]). This could make confusion in case of a real structure for which the location of faults is not known in advance. To investigate the accuracy of equation (1), the finite element solution of the *MC* is calculated by using the following expression

$$v'' = M/EI. \tag{2}$$

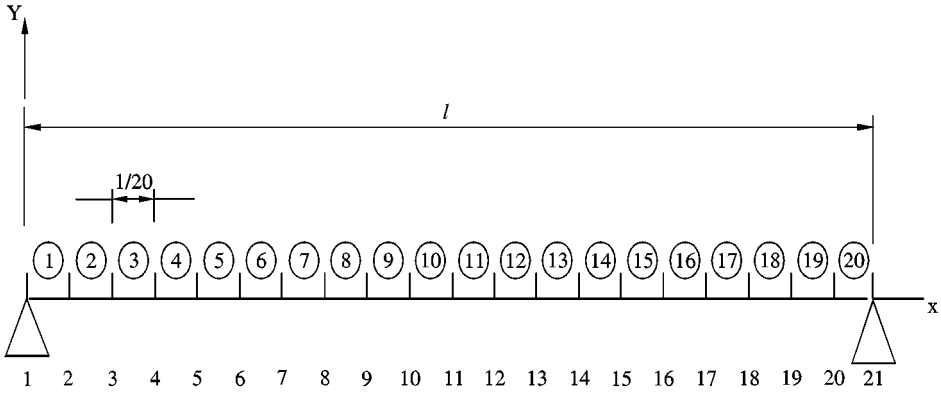

Figure 1. Finite element model—simply supported beam ($1 = 6$ m, $A = 0{\cdot}09$ m^2, $\rho = 2500$ kg/m^3. EI $= 20{\cdot}25 \times 10^6$ N m^2).

TABLE 1

Comparison of natural frequencies—simply supported beam (*reduction of* 90% *in EI at element* 10)

Mode	Frequency (Hz)		% difference
	Intact beam	Damaged beam	
1	14·124	10·24	27·5
2	56·324	55·771	0·98
3	126·092	104·202	17·36
4	222·613	216·203	2·88
5	312·125	304·664	3·7

The bending moment M for each node is directly calculated in the finite element solution for the intact and the damaged beam. It should be noted that for real experimental measurements only equation (1) is applicable.

The natural frequencies of the intact and the damaged simple beam are given in Table 1 for the first five modes. The results indicate the presence of damage in a global sense but cannot localize it without further analysis. Figure 2 summarizes the mode shape of the first five modes of the intact beam. It has been found [5] that the Modal Assurance Criterion (MAC) [19] and the Co-ordinate Modal Assurance Criterion (COMAC) [20] are not sensitive to damage and therefore they will not be considered in the current study. The absolute difference between the modal curvature of the intact and the damaged beam is plotted in Figure 3 by using

Figure 3. Absolute difference in MC—simple beam model —20-element model—90% reduction in EI at element 10. —◆— equation (1); —▲— equation (2). (a) mode 1; (b) mode 2; (c) mode 3; (d) mode 4; (e) mode 5.

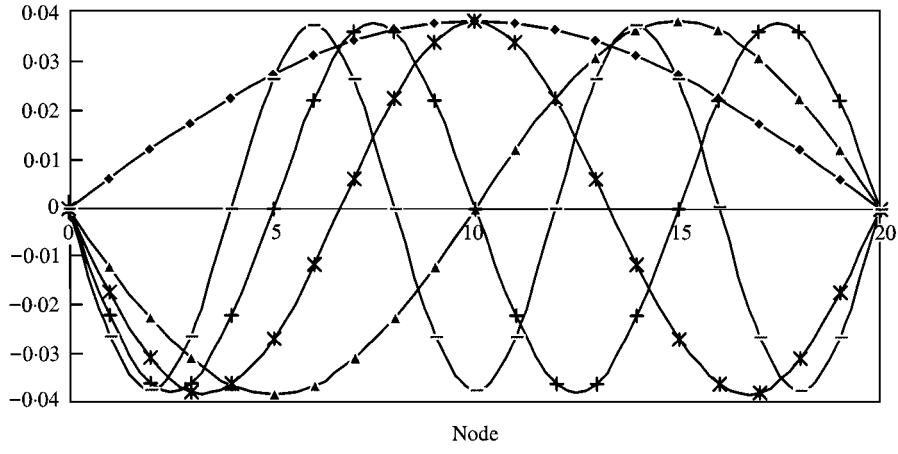

Figure 2. Mode shapes—simply supported beam. —◆— mode 1; —▲— mode 2; —*— mode 3; —+— mode 4; ——— mode 5.

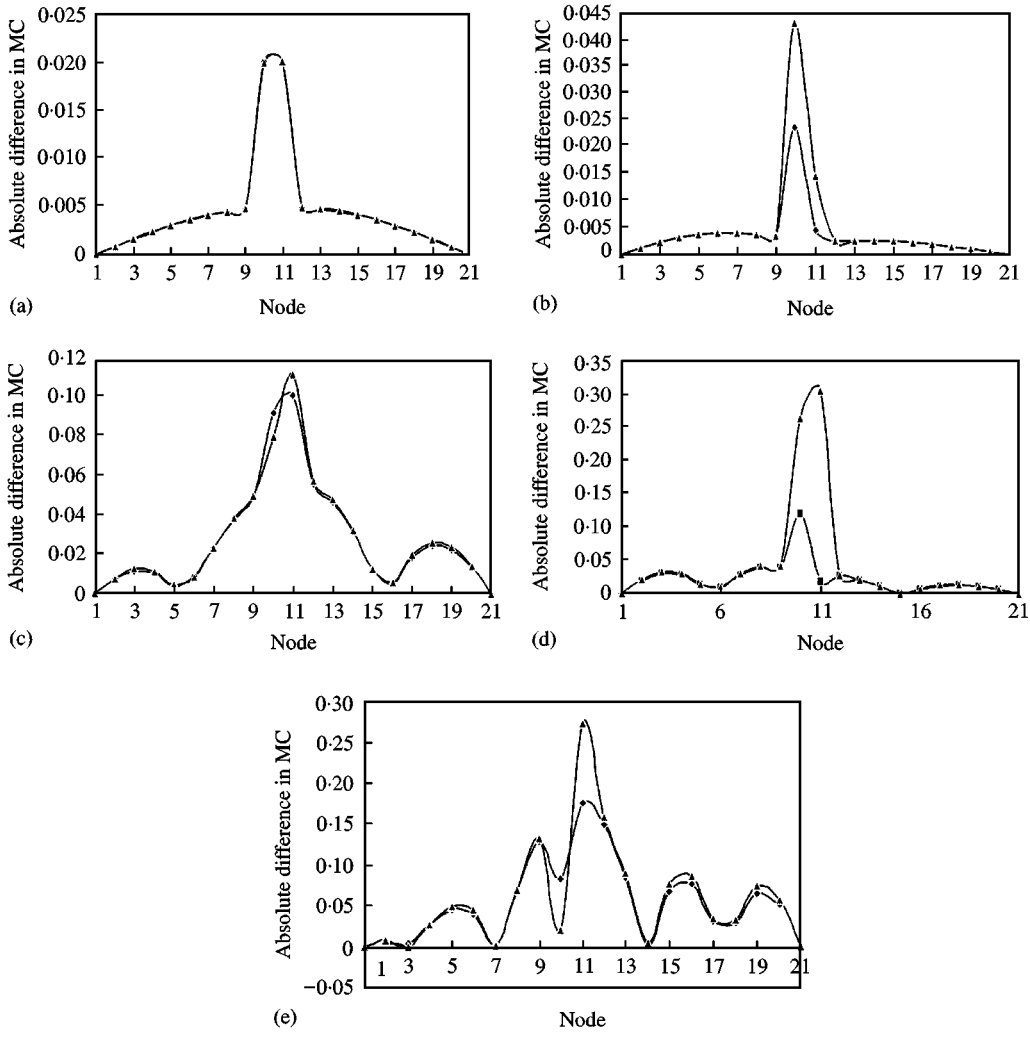

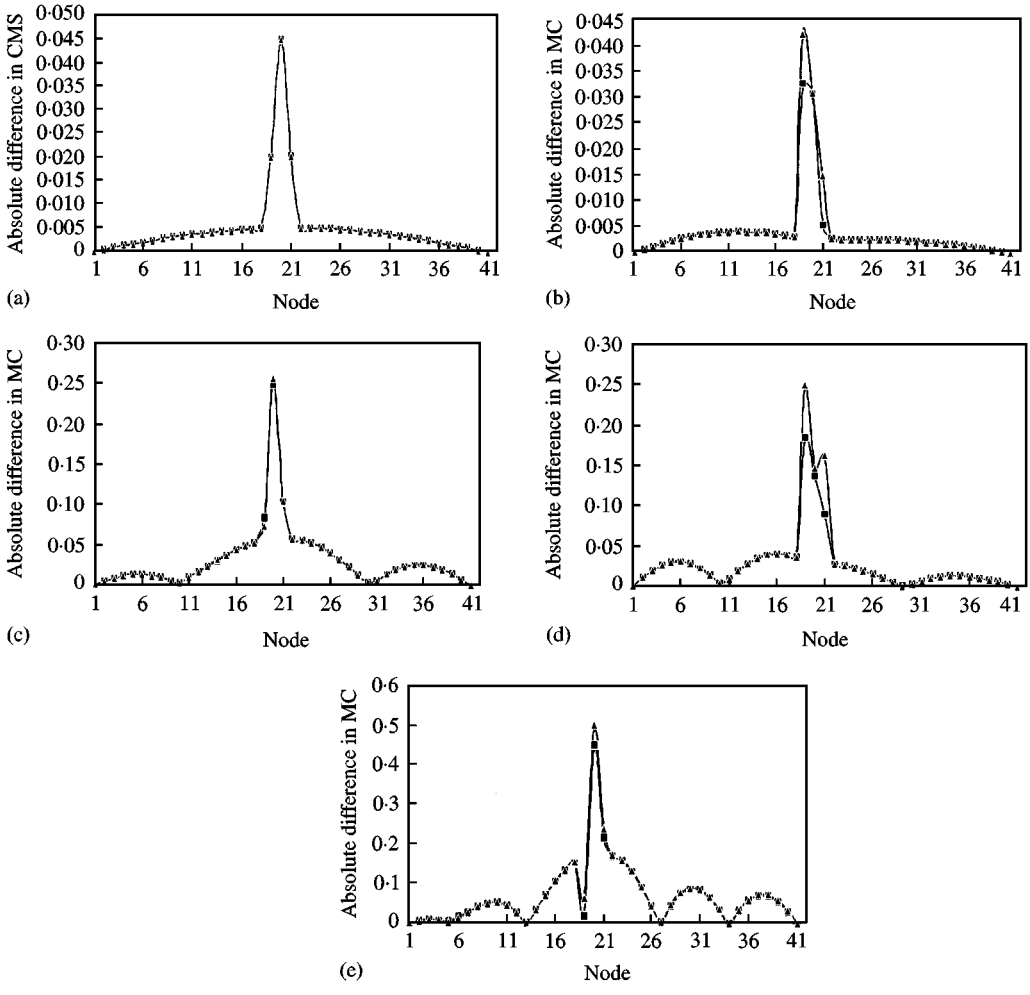

Figure 4. Absolute difference in *MC*—simple beam model —40-element model. —◆— equation (1); —▲— equation (2). (a) mode 1; (b) mode 2; (c) mode 3; (d) mode 4; (e) mode 5.

equations (1) and (2). It can be observed that the *MC* of the higher mode are less accurately determined than the first one when using equation (2). For the higher modes (especially mode 5), the difference in *MC* shows several peaks not only at the position of the damaged element but also at other positions regardless which equation is used. The size of the fault remains the same as in the former mesh. The difference in *MC* for the refined mesh are plotted in Figure 4. The accuracy of the central difference approximation (equation (1)) is improved for the 40-element model. Good agreement between equations (1) and (2) can be observed from Figure 4. The agreement between both equations is perfect for the first mode. The undesirable and misleading peaks for the higher modes (in Figure 3) are now reduce in the 40-element model (Figure 4). It is obvious then that in order to derive the *MC* correctly for the higher modes, a fine mesh is required. Because in practical

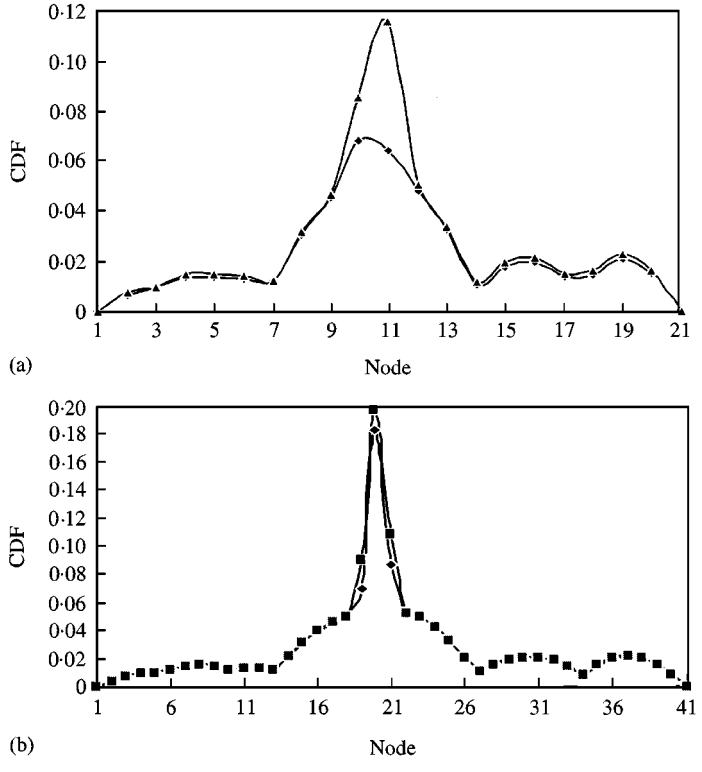

Figure 5. Curvature damage factor (*CDF*)-simple beam model; (a) 20-element; (b) 40-element; —▲—, equation (1); —■—, equation (2).

application the number of sensors is limited, the first mode will provide the most reliable *MC*.

Now, to summarize the results for all modes, the "curvature damage factor" is proposed as

$$CDF = \frac{1}{N} \sum_{n=1}^{N} |v''_{o_i} - v''_{d_i}|, \tag{3}$$

where N is the total number of modes to be considered, v''_0 is the curvature mode shape of the intact structure and v''_d is that of the damaged structure.

Figure 5 shows the "*CDF*" for the simple beam when using the 20-element and the 40-element models. The position of damage is clear from Figure 5 (*CDF*). Obviously, the 40-element model gives more clear peaks at the position of damage than the 20-element model especially when using the central difference approximation (equation (1)).

2.2. CONTINUOUS BEAM

To examine the above technique for beams with more than one span having several damage locations, which is the case of a bridge, a two-span beam is

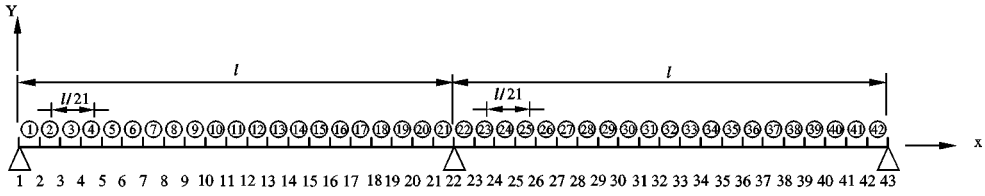

Figure 6. Finite element mesh—continuous beam model ($l = 6{\cdot}3$ m, $A = 0{\cdot}09$ m^2, $\rho = 2500$ kg/m^3, $EI = 20{\cdot}25 \times 10^6$ Nm^2)

TABLE 2

Comparison of natural frequencies—continuous beam model

Mode	Frequency (Hz)		% difference
	Intact beam	Damaged beam	
1	12·812	12·239	4·4
2	20·012	18·146	9·38
3	51·107	51·017	0·017
4	64·662	61·273	5·24
5	114·465	109·477	4·35

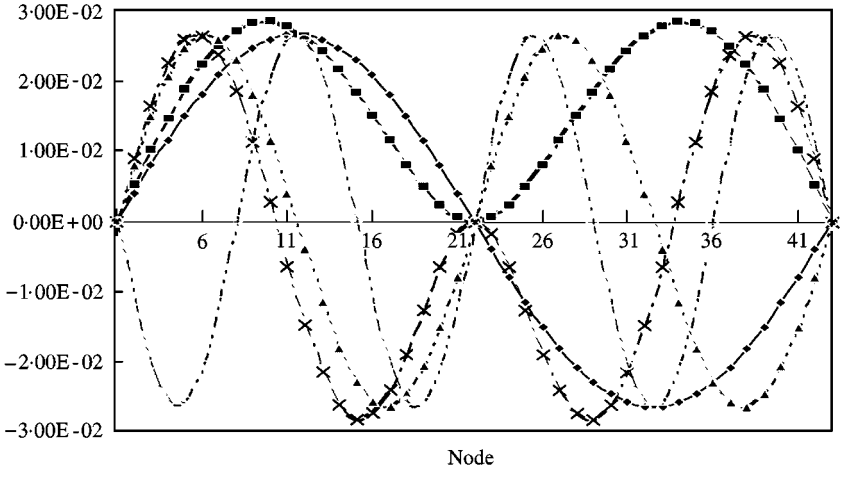

Figure 7. Mode shapes-continuous beam. Mode no.: —◆—, 1; —■—, 2; —▲—, 3; —×—, 4; –·–·–, 5.

considered. The beam is discretized by 42 elements (21 elements over each span). The finite element mesh for this continuous beam is shown in Figure 6. Three damage locations are assumed at the middle of each span (elements 11 and 32) and at the intermediate support (elements 21 and 22). The stiffness of the beam is reduced by 50% over these elements at those three positions. Table 2 compares the natural frequencies of the intact and the damaged beam for the first five modes. The

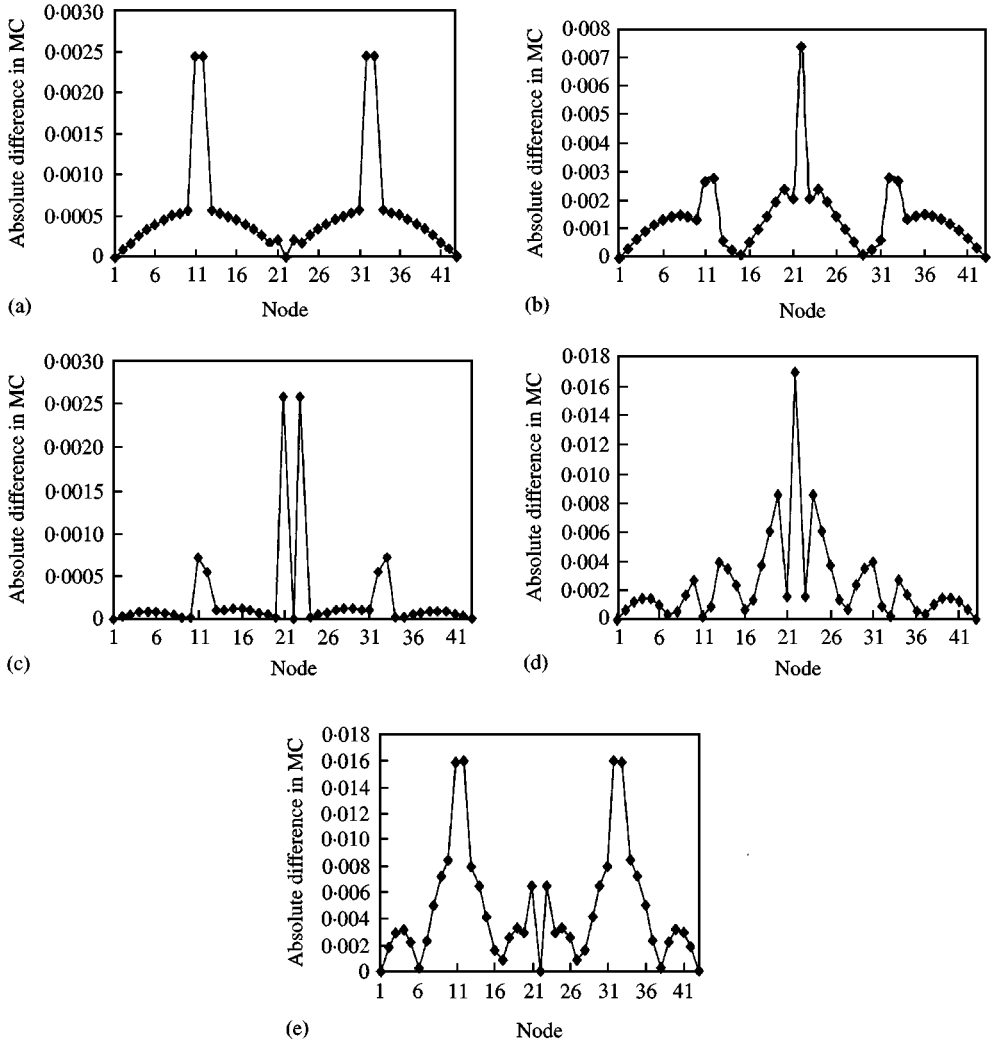

Figure 8. Absolute difference in MC-continuous beam. Mode no: (a), 1; (b), 2; (c), 3; (d), 4; (e), 5.

percentage difference between the natural frequencies of the intact and the damage beam varies for different modes. Again, this comparison indicates the presence of faults, but to localize them the difference in MC should be plotted. The first five displacement mode shapes are shown in Figure 7. The difference in MC between the intact and the damaged continuous beam is plotted in Figure 8 for the first five modes. For the first mode [Figure 8(a)], it can be observed that the peak at the intermediate support is very small comparing to that at the middle of each span. In fact, for mode 1 the MC at this support is zero and has very small values at the nodes next to it. In contrast, at the middle spans high MC takes place. The same remark can be observed for mode 5 [Figure 8(e)]. On contrary, modes 2 and 4 [Figures 8(b) and (d)] show a high difference in MC peak at the intermediate

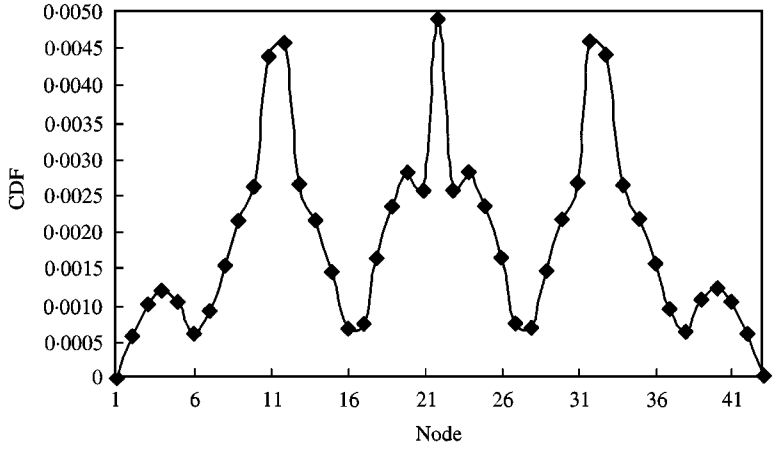

Figure 9. CDF-continuous beam.

support and small peaks at the two middle spans. The *MC* at the intermediate support is much higher than that at the middle spans for those modes. Depending on the absolute ratio between the *MC* values for a particular mode at two different locations, one peak can dominate the other. Therefore, one can conclude that in case of several damage location in a structure, all modes should be carefully examined.

The "*CDF*" is calculated for the five modes and plotted in Figure 9. Because *CDF* is nothing more than averaging the absolute difference in CMS over all modes, it seems to be a good indicator for damage localization especially when several faults are presented in the structure.

3. APPLICATION: BRIDGE Z24

3.1. DESCRIPTION OF THE BRIDGE

The bridge Z24 lies over the highway A1 (Bern/Zurich) and connects the two villages Koppigen and Utzenstorf. It was built during the early 1960s. Figure 10 shows a top and bottom view of the Z24. A sketch of the bridge from different views is illustrated in Figure 11. The total length of the bridge is 63·4 m [as shown in Figure 11(b)]; two side spans of 14 m each, 30 m mid-span and two cantilevers of 2·7 m each. The cross-section of the bridge girder consists of two box cells [Figure 11(c)]. The post-tensioning cables are located in the three webs. The total number of wires is 16 and carries a total force of 2460 t. Two piers and two abutment columns [Figure 11(a)] support the superstructure. The girder is rigidly connected to the two piers and connected through concrete hinges to the columns. The bridge has a small skewness angle as shown in Figure 11(d). The columns and the two cantilevers ends are completely embedded in the soil.

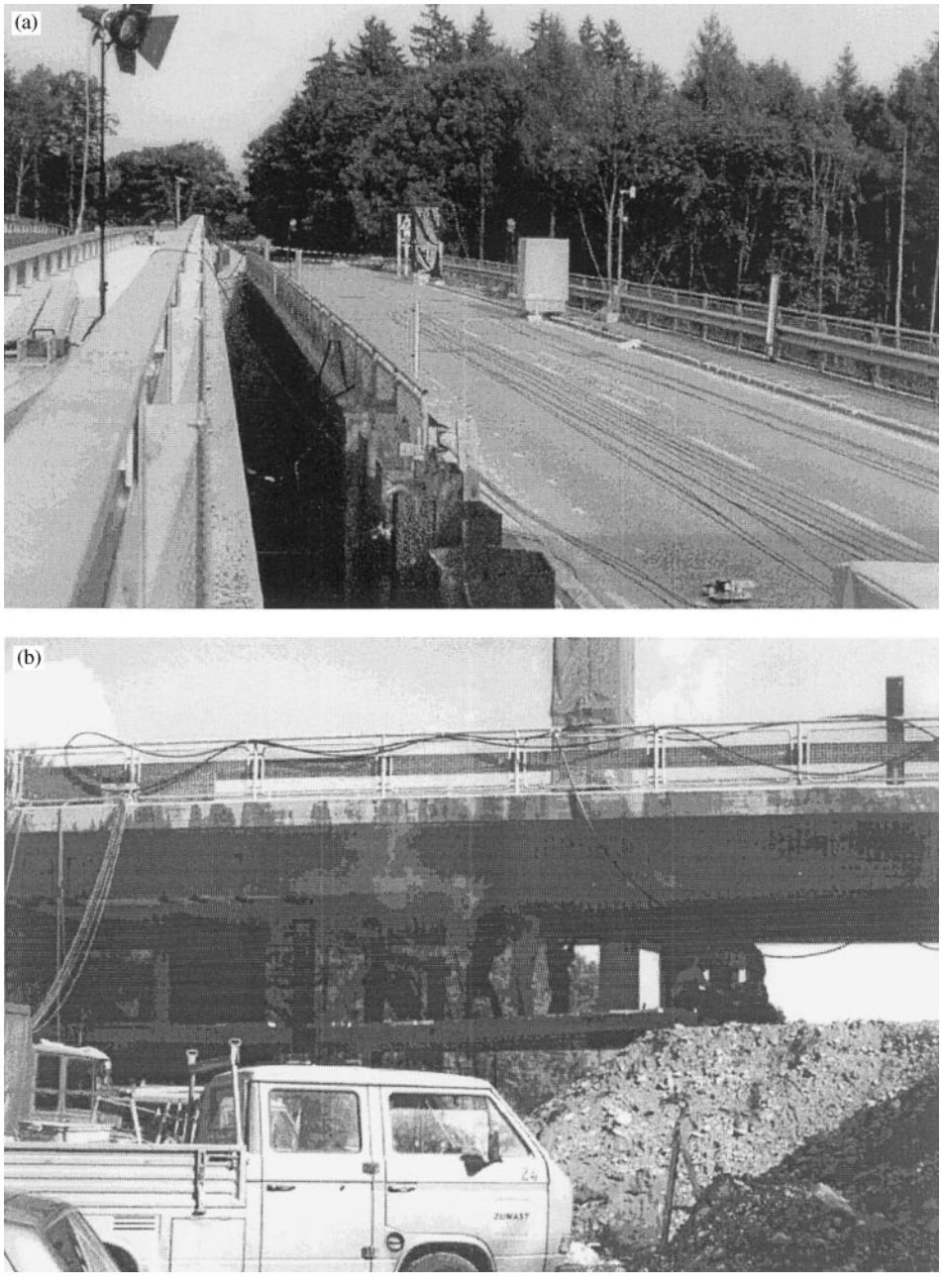

Figure 10. Bridge Z24, (a) top view, (b) bottom view.

3.2. DAMAGE SCENARIO: SETTLEMENT OF PIER

A settlement is applied to the pier at side Koppigen [see Figure 11(b)]. To allow for a settlement, the pier was cut, some part of the concrete was removed and replaced by steel fill plates and three hydraulic jacks as illustrated in Figure 12 (see

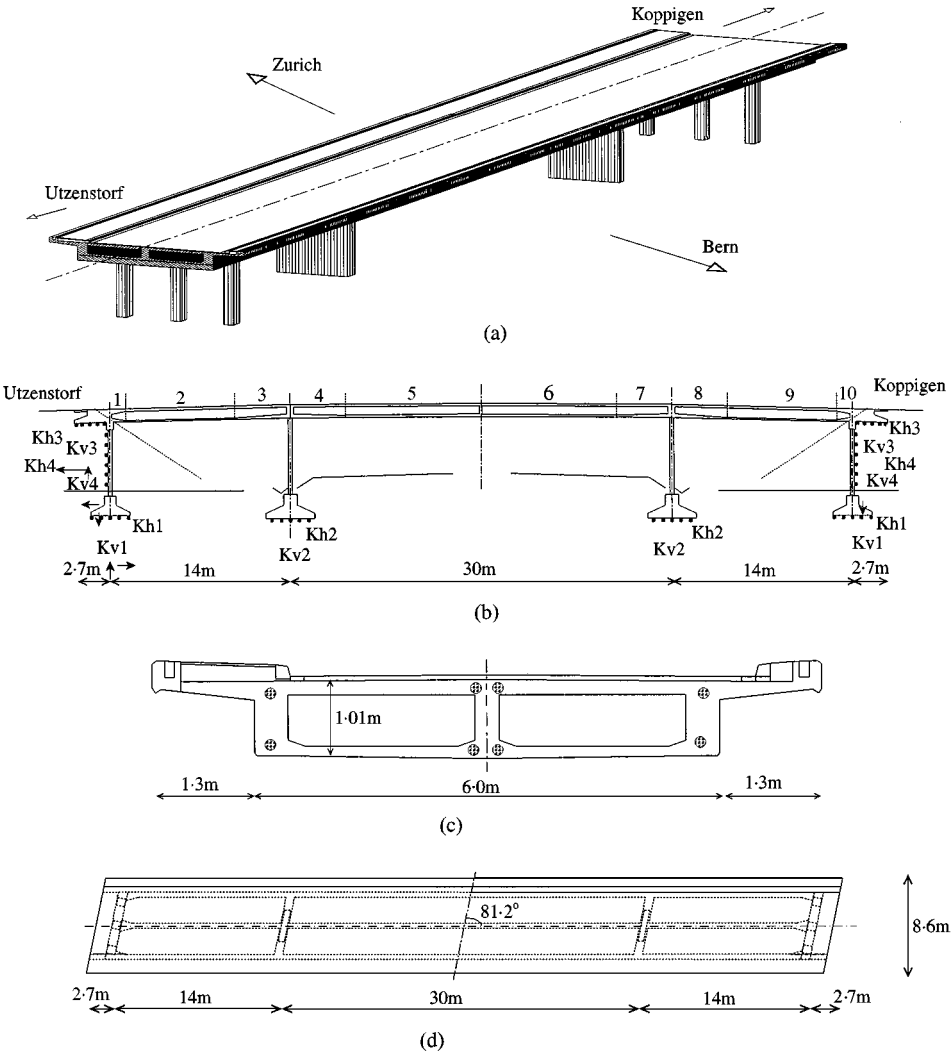

Figure 11. Sketch of bridge Z24. (a), Global view; (b), elevation; (c), cross-section; (d), 4; (e), 5.

reference [16] for more details). The jacks allow for lowering and lifting the pier. The settlement scenario was realized in different steps (20, 40, 80 and 95 mm). After each step, dynamic measurements were carried out using ambient vibration due to the traffic under the bridge (on the highway A1). Three rows of measured points (side Bern, the middle and side Zurich) are considered along the whole bridge length, each of 3 measured points. Table 3 summarizes the first four natural frequencies measured after each damage step and compares them to the reference measurement.

As can be seen from Table 3, the scenarios settlement 80 and 95 mm show considerable change in natural frequencies (modes 1, 3 and 4) when compared to the reference results. Because mode 2 is a horizontal mode, it is not affected by

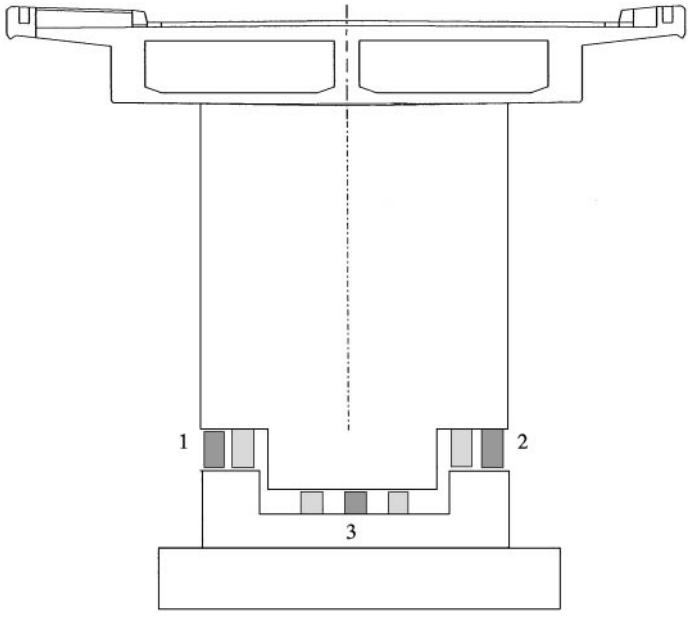

Figure 12. Installation of settlement system at pier Koppigen. ■ Jack; □ Steel plates.

TABLE 3

*Natural frequencies for the scenario settlement of pier — bridge Z*24

Date	Description	Natural frequencies (Hz)			
		1	2	3	4
09/08/98	Reference	3·88	5·01	9·80	10·3
10/08/98	Settlement 20 mm	3·87	5·06	9·79	10·32
12/08/98	Settlement 40 mm	3·86	4·93	9·74	10·25
17/08/98	Settlement 80 mm	3·76	5·00	9·37	9·90
18/08/98	Settlement 95 mm	3·67	4·94	9·21	9·68

damage. The settlements 20 and 40 mm show very little change in natural frequencies, which indicates that the bridge is not yet damaged. This is in agreement with what has been observed during the realization of the settlement scenario: cracks are initiated in the girder at pier Koppigen at a settlement of about 60 mm. For the case of 80 and 95 mm settlement, a cracked zone of about 10 m left and right of the pier Koppigen was noticeable.

Now, to detect the location of damage in the bridge using the change in MC, one considers that the reference measurement represents the intact bridge (the reference test was performed one day before applying any damage to the bridge). The damaged state is represented by the dynamic measurements carried out after applying a settlement scenario (80 or 95 mm). The main difficulty in computing MC

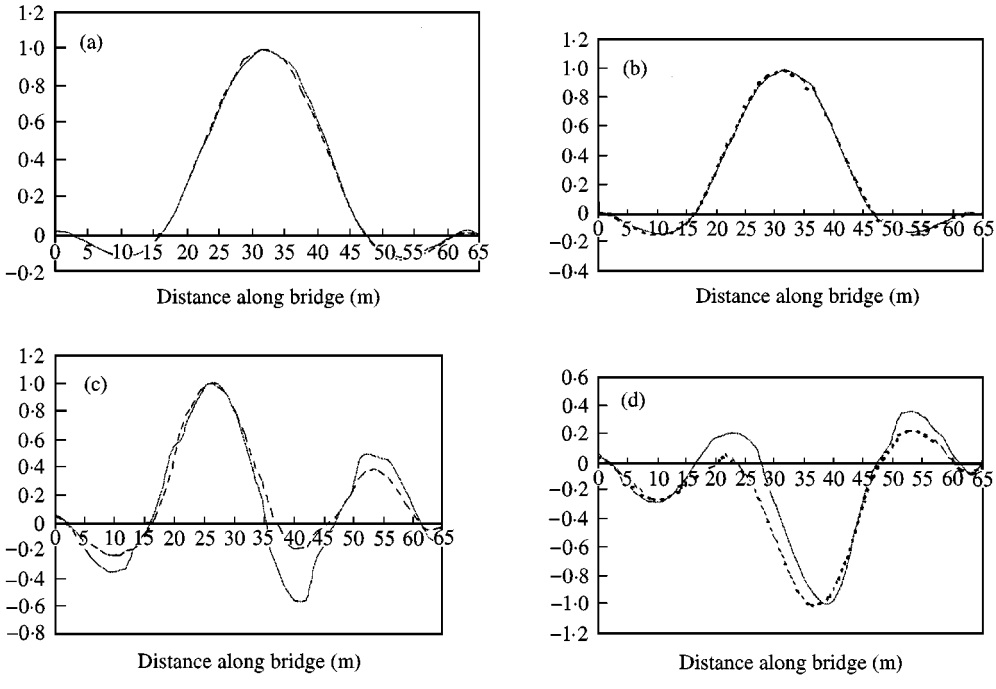

Figure 13. Comparison of mode shapes. ---- Reference, —— settlement 80 mm. (a) mode 1, side Bern, (b) mode 1, side Zurich; (c) mode 3, side Bern; (d) mode 3, side Zurich.

from the experimental data lies in the fact that the measured mode shapes can never be perfectly smooth. In turn, by using the central difference approximation (equation (1)), the computed *MC* will show irregular variation. To overcome this problem, the measured mode shapes are smoothed by using curve fitting analysis before using them in equation (1) to calculate the *MC*. In order to obtain good smoothing curves for the mode shapes, a high order polynomial is required. A six degree polynomial is applied to every 10 measured points. Figures 13 and 14 show the measured mode shapes, the absolute difference in *MC* and the "*CDF*" for the scenario settlement 80 mm for modes 1 and 3. Similar results are plotted in Figures 15 and 16 for the case of settlement 95 mm.

For scenario settlement 80 mm, the first measured mode shape is smoother than the third one (Figure 13), and gives a more clear indication at the position of damage [Figures 14(a)–(c)]. Due to the high irregularities in the measured mode shape 3, the location of damage cannot be identified form Figure 14(c) and (d). It should be noted that because there is a point of zero curvature (for modes 1 and 3) near the pier, two peaks in the difference in *MC* should appear in the damage zone. In calculating the *CDF* [equation (3)], the two sides (side Bern and side Zurich) are considered.

For the case of settlement 95 mm, the quality of the measured mode 3 is much better than that of the previous case. Therefore, good localization of damage can be done from Figure 16 from the results of both modes 1 and 3. The Curvature Damage Factor shows two peaks at the pier Koppigen [Figure 16(e)].

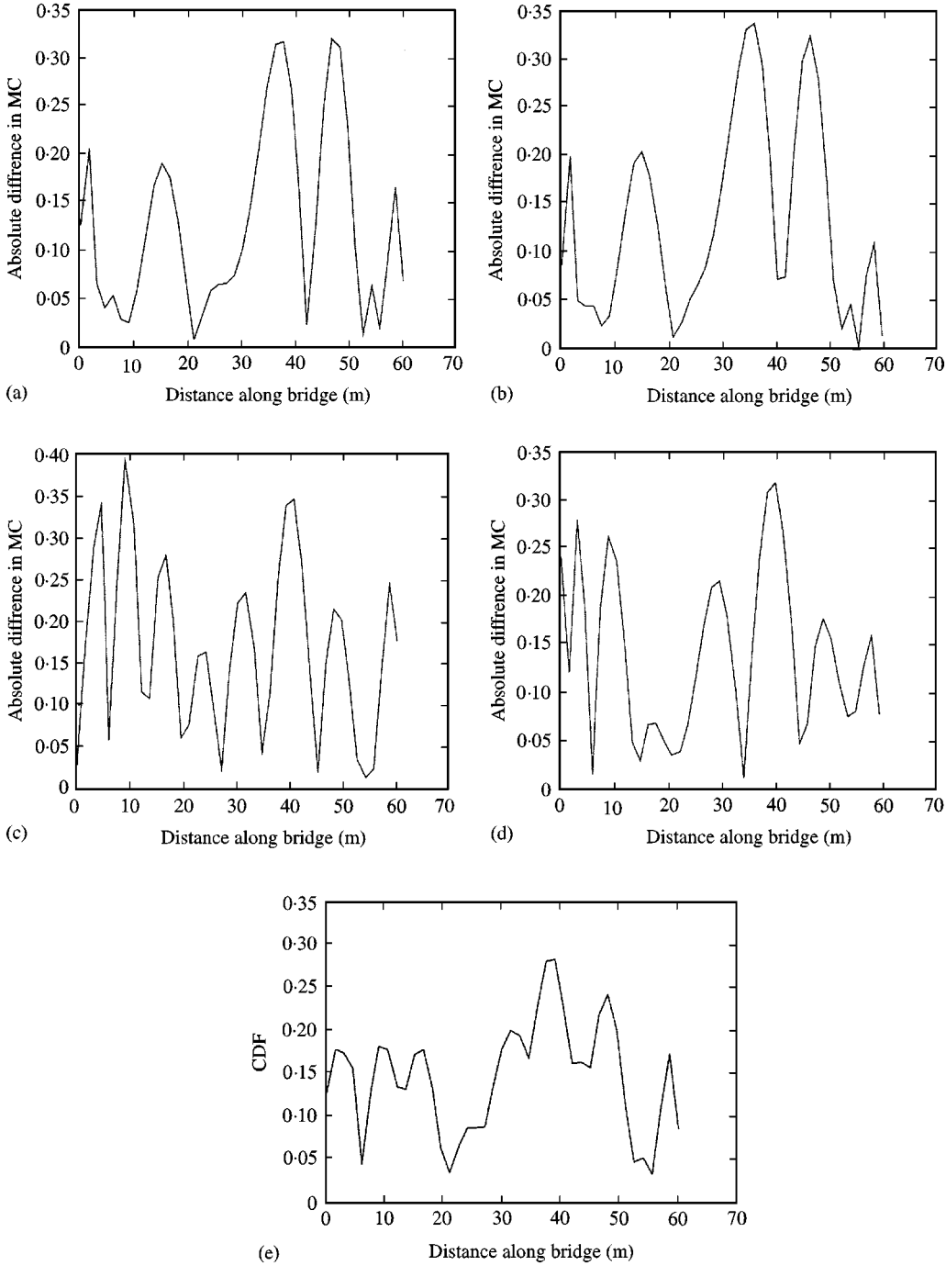

Figure 14. Difference in *MC* and *CDF*—settlement 80 mm. (a) Mode 1, side Bern, (b) mode 1, side Zurich; (c) mode 3, side Bern; (d) mode 3, side Zurich; (e) *CDF*; (e) curvature damage function.

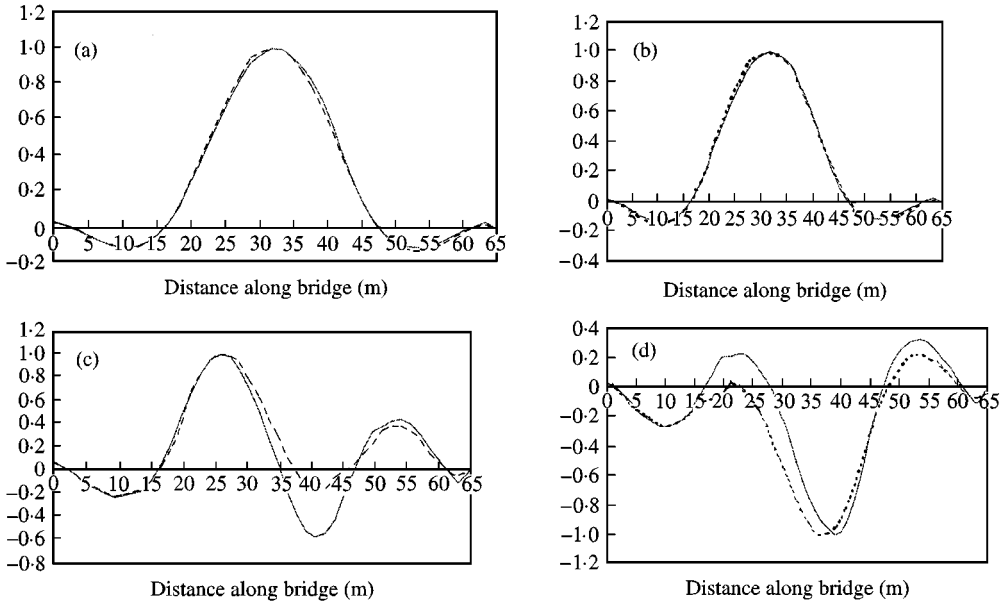

Figure 15. Comparison of mode shapes. ---- Reference, —— Settlement 95 mm. (a) mode 1, side Bern, (b) mode 1, side Zurich; (c) mode 3, side Bern; (d) mode 3, side Zurich.

4. CONCLUSION

The modal curvature (*MC*) technique for damage localization in structures is investigated in this paper. A theoretical study using simulated data for a simple and a continuous beam has been conducted. The modal curvatures of the lower modes are in general more accurate than those of the higher ones. An extensive measurement grid is required in order to get a good estimation for the higher *MC*. When more than one fault exists in the structure, it is not possible to locate damage in all positions from the results of only one mode. All modes should be carefully examined in order to locate all existing faults. A new parameter called "*CDF*" (*CDF*) is introduced, in which the difference in *MC* is averaged over all modes. When the structure contains several damage locations, the *CDF* gives a clear identification of these locations.

The *MC* technique is further applied to a really measured data on a prestressed concrete bridge, Z24. Due to the irregularities in the measured mode shapes, a curve fitting has to be applied before calculating the *MC* using the central difference approximation. The results confirm that the application of the *MC* method to detect damage in civil engineering structures seems to be promising. Techniques for improving the quality of the measured mode shapes are highly recommended. Care should be exercised when using the *MC* of higher modes for the purpose of damage detection.

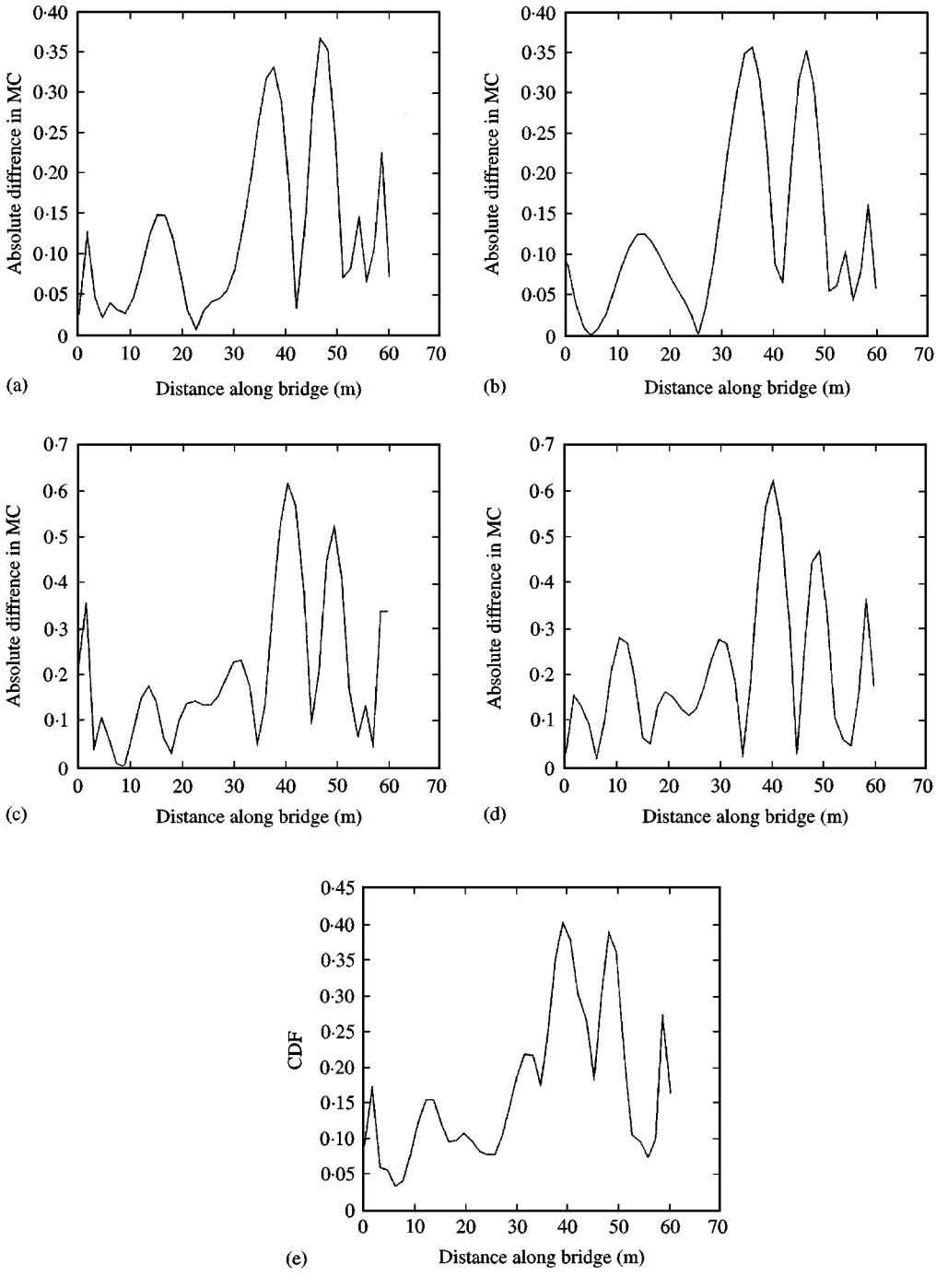

Figure 16. Difference in *MC* and *CDF*—settlement 80 mm. (a) Mode 1, side Bern, (b) mode 1, side Zurich; (c) mode 3, side Bern; (d) mode 3, side Zurich; (e) *CDF*; (e) curvature damage function.

ACKNOWLEDGMENT

The controversial nature of the modal methods of damage assessment of civil engineering structures among practitioners is highly acknowledged.

Thanks goes to engineers Hans Desmedt and Roelnd Engelen for the preliminary work in this area at the Department of Civil Engineering, KU Leuven.

The damage scenarios on bridge Z24 were realized by the EMPA team, engineers C. Kramer, C. de Smet and S. Olia.

The research has been carried out in the framework of the BRITE-EURAM Programme CT96 0277, SIMCES with a financial contribution by the Commission.

Partners in the project were: K. U. Leuven (Department Civil Engineering, Afdeling Bouwmechanica); Aalborg University (Institut for Bygningsteknik): EMPA (Swis Federal Laboratories for Materials Testing and Research, Section Concrete Structures); LMS (Leuven Measurements and Systems International N. V., Engineering and Modeling); WS Atkins Consultants Ltd. (Science and Technology); Sineco Spa (Ufficio Promozione e Sviluppo); and Technische Universitä Graz (Structural Concrete Institute).

REFERENCES

1. R. D. Adams, D. Walton, J. E. Flitcroft and D. Short, 1975, *Composite Reliability*, *ASTMSTP* **580**, 159–175. Philadelphia: American Society for Testing and Materials. Vibration testing as a nondestructive test tool for composite materials.
2. O. Loland and C. J. Dodds, 1976 *Proceedings of the Eighth Annual Offshore Technology Conference*, Vol. 2, 331–3319. *OTC Paper No.* 2551. Experiences in developing and operating integrity monitoring system in north sea.
3. J. K. Vandiver, 1975 *Proceedings of the Seventh Annual Offshore Technology Conference* **2**, 243–252, Detection of structural failure on fixed platforms by measurements of dynamic response, OTC, Paper No 2267. Vibration Engineering 973–982. Error localization using power spectral densities.
4. A. Nauerz and C. P. Fritzen 1996, The *21th International Seminar on Modal Analysis* (*ISMA 21*), *Noise and Vibration Engineering* 973–982. Error localization using power spectral densities.
5. A. K. Pandey, M. Biswas and M. M. Samman 1991 *Journal of Sound and Vibration* **145**, 312–332. Damage detection from changes in curvature mode shapes.
6. C. Williams and O. S. Salawu 1994 *Bridge Assessment Management and Design* (B. I. G. Barr *et al*., editors London: Elsevier. Concepts of condition assessment of bridges using vibration testing and analysis.
7. C. Sikorsky and N. Stubbs 1997 *Structural Damage Assessment Using Advanced Signal Processing Procedures*, 399–408. Sheffeld University Press. Improving bridge management using NDT and quality management.
8. C. Farrar and D. Jauregai 1996 *Technical Report*, *LA-1304-MS*, *Los Alamos*, *National Laboratory*. Damage detection algorithms applied to experimental and numerical modal data from the 1–40 bridge.
9. M. M. Abdel Wahab, G. De Roeck and B. Peeters 1999 *Proceedings of the International Conference on Identification in Engineering Systems. University of Wales Swansea*, *U.K.* 29–31 *March.* On the application of FE model updating to damaged concrete beams.
10. H. Ahmadian, J. E. Mottershed and M. I. Friswell 1996 The *21th International Seminar on Modal Analysis* (*ISMA 21*), *Noise and Vibration Engineering* 983–991. Damage detection from substructure modes.

11. H. G. Nake and C. Cempel 1991 *Mechanical Systems and Signal Processing* 345–359. Fault detection and localization in structures: a discussion.
12. P. Hajela and F. J. Soeiro 1990 *AIAA Journal* **28**, 1110–1115. Structural damage detection based on static and modal analysis.
13. D. C. Zimmerman and M. Kaouk 1994 *Journal of Vibration and Acoustics* **116**, 222–231. Structural damage detection using a minimum rank updating theory.
14. M. I. Friswell and J. E. Mottershead 1995 Finite Element Model Updating in Structural Dynamics. Dordrecht, The Netherlands. KLUWER Academic Publisher.
15. *Brite EuRam BE96-3157-SIMCES*. Project programme, 1996.
16. C. Kramer C. A. M. De Smet and G. De Roeck 1999 *Proceedings of International Modal Analysis Conference IMAC99. Kissimmee, FL 8–11 February*. Z24 bridge damage detection tests.
17. M. M. Abdel Wahab, J. Maeck and G. De Roeck 1999 *Proceedings of International Modal Analysis Conference IMAC99. Kissimmee, FL 8–11 February*. Numerical simulation of damage scenarios of bridge Z24.
18. M. M. Abdel Wahab 1998 *Technical Report*, K. U. Leuven, July. Finite element simulation of damage scenarios of bridge Z24.
19. R. J. Allemang and D. L. Brown 1982 *First International Modal Analysis Conference*. Orlando, Florida, 110–116. A correlation coefficient for modal vector analysis.
20. N. A. J. Lieven and D. J. Ewins 1988 *Proceedings of the sixth International Modal Analysis Conference*, 690–695. Spatial correlation of mode shapes, the Co-ordinate Modal Assurance Criterion (COMAC).